

## AN EXPERIMENTAL STUDY OF LOW-CURRENT DC SERIES ARC FAULTS FOR CONDITION MONITORING PURPOSE

Shibo Lu, B. T. Phung, Daming Zhang, and Hua Chai

School of Electrical Engineering and Telecommunications, University of New South Wales, Sydney, Australia  
shibo.lu@unsw.edu.au

### ABSTRACT

*DC arc faults present a challenging protection problem in DC systems, such as photovoltaic and electric vehicle supply systems. Incidents of DC arc faults in DC systems are becoming more common especially for series arc faults, and if undetected, would finally cause severe damage to the systems. This paper studies DC series arc fault characteristics including quasi-stationary V-I characteristic and arc current spectrum characteristic. Based on experimental tests, the impacts of different load current levels, DC operating voltage levels, air gap lengths on arc current and its spectrum are investigated and evaluated. A new method based on wavelet packet decomposition combined with entropy theory has been developed to extract the common features of arc signals under different conditions. It is found that arc fault currents share some common wavelet-packet entropy in different bandwidths even if the fault conditions are different. The results provide better characterization of DC arcing phenomena and help to develop more effective detection algorithms.*

### INTRODUCTION

With rapidly growing deployment of DC systems worldwide, DC arc fault protection is becoming increasingly important for delivering electricity in a safe and reliable manner. Unlike AC arc faults, the absence of current zero-crossing makes DC arc fault more sustainable and difficult to be suppressed. DC arc fault can happen in DC systems with different voltage levels, such as 270 V electrical aircraft systems, 380 V DC distribution systems, photovoltaic (PV) systems ranging from tens to hundreds of volts [1-2]. There is an increasing risk of DC arc faults because of the increasing DC operating voltage levels. If an arcing incident remains undetected, it will ignite and burn surrounding materials and finally leading to a fire. Therefore, such a dangerous event is required to be detected and interrupted at its early stage.

The high-frequency variations are related to cathode spot activities. The reason is cathode spot motion can cause localized breakdown in the plasma sheath, which can generate broadband of RF signals. Focusing on the Radio Frequency (RF) current with frequency up to tens of MHz requires high-performance sensors and measurement equipment to precisely capture the high frequency components. It also requires a more powerful and costly microcontroller to process large amount of data under the higher sampling rate. Furthermore, the behaviors of RF current, especially above 100 kHz, can be affected by various factors in PV systems [3]. Therefore, this research is focused on the frequency contents below 100 kHz.

Voltage-current characteristics of arcing fault have been studied over past few decades, and many empirical equations have been proposed to describe the static V-I characteristics [3]. However, behaviors of the high frequency components of the arc current and their dependency on many other factors are often ignored. Yao et al. proposed a discrete wavelet transform (DWT) based algorithm and it achieves 100% accuracy at lower current and voltage level, while the accuracy decreases significantly at higher current and voltage level [1]. In [4], the sum of power spectrum components in the 40-100 kHz frequency band has been used as an indicator, which increases after arc fault occurrence. However, the algorithm may fail at higher current level: it has been shown that, under fixed source voltage and gap distance, the probability distribution of arcing signal can extend into the area of normal signal at higher load current level. This can affect the detection accuracy and reliability of the detection algorithm [5]. Furthermore, Zhen et al. found that fault indicator with satisfactory performance for 28V DC systems may fail to work for 270V DC systems under the same load current [6]. Therefore, high frequency noise characteristics play an important role in the development of arc fault detection algorithms. All these factors call for a more in-depth understanding of DC arc fault phenomenon to achieve better detection.

A preliminary study can be found in [7] but further investigations need to be carried out. This research presents a comprehensive experimental study to understand low-current DC series arc fault behaviors in DC networks from two different viewpoints: quasi-stationary characteristics and arc noise. It is found that high frequency components of the arc current show dependency on the load current level, source voltage level, and gap length. Furthermore, based on experimental results, the arc process can be generalized in 3 different phases and the degree of variation in high-frequency components of the current is different. The higher the load current, the faster the arc reaches the final phase. As arc fault shows different behavior at different working condition, a method is needed to extract the consistent features. Based on analysis of experimental results, wavelet packet entropy shows good performance.

### EXPERIMENT SETUP AND PROCEDURE

The power source is LAB/HP 15600, and an adjustable resistance bank with up to 85.5Ω is used as load. The DC information of the loop current and arc voltage is captured by PROSyS-CP35 differential current probe and SI-9000 differential voltage probe, respectively. In addition, the high frequency variation of the loop current is captured by a Pearson-4688 current transformer with 600 Hz cutoff frequency (-3dB attenuation). The data acquisition (DAQ) system consists of a National Instruments PXIe-1073 and

a PXIe-4300. The PXIe-4300 can stream the raw data to the computer at the maximum sampling frequency of 200 kHz. The experimental setup is shown in Figure 1. Copper electrodes of 6.4 mm diameter with flat tip are used in this paper. The experimental conditions are listed in Table 1. The same data collection procedures are followed for all experimental conditions: (1) wait until electrodes and load resistor cool down to the ambient temperature; (2) polish electrodes with sand paper, mount electrodes onto the arc generator, and connect them together; (3) adjust the load resistance; (4) start the DC power source and adjust the voltage and current to the desired level; (5) start the data acquisition (DAQ) system in PC; (6) pull apart copper electrodes to initiate an arc and adjust the gap length to the desired value; (7) shut down the DC power source to extinguish the arc and stop the measurement. All the data sets are saved locally. Then, the on-site data sets are visualized, analyzed, and processed by Matlab.

## STATIC CHARACTERISTICS OF DC ARCING

### V-I Characteristics

Arcing is a very complex physical phenomenon. Nowadays, most arc studies are based on observation of experiments and analysis of acquired data, and scholars mainly use the V-I curve to characterize this phenomenon [3, 8]. The arc can be then treated as a non-linear resistance. In this paper, the experimental data is fitted to the Nottingham arc model, which is suitable for gap length from 1mm to 10 mm, shown as follows in Eq. (1):

$$V_{arc} = A + \frac{B}{I_{arc}^n} \quad (1)$$

where  $A$ ,  $B$ , and  $n$  are arc constants depending on gap

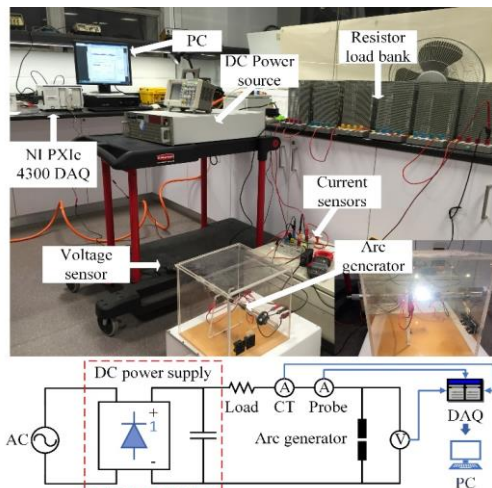


Figure 1: Experimental setup

Table 1: Experimental conditions

Case	Condition (air gap width = 1, 2, 3 mm)
Fixed DC voltage (200V)	4.1, 7.9, 11, 13.6 A
Fixed DC current (6.5A)	87, 111, 134, 158 V

length. The result is illustrated in Fig. 2, and it is consistent with the results in [8], which validate the accuracy of our experimental works. It should be noted that the arc gap length is not equal to actual arc length, and the additional impedance injected into the circuit is contributed by the arc length; however, it could be considered they are the same when the air gap length is small, which is the case in this research. The effects of air gap length can be obtained from Fig. 2. If assuming the electrical conductivity and the effective cross-section area of the arc column remain the same in the quasi-stationary state, the arc resistance is proportional to length according to (2):

$$R_{arc} = \frac{1}{\sigma} \frac{l}{S} \quad (2)$$

where  $\sigma$  is electrical conductivity of the arc column,  $l$  is arc length (it equals gap length for short arc), and  $S$  is the effective cross-section area of the arc column.

### Stable Operating Point

In a typical DC circuit, the following equation can be obtained:

$$V_{source} = L_{load} \frac{dI}{dt} + R_{load}I + V_{arc} \quad (3)$$

where  $V_{source}$  is DC source voltage,  $R_{load}$  and  $L_{load}$  are circuit parameters, and  $V_{arc}$  is the arc voltage, which equals to 0 before arc fault instant. Equation (3) can be rewritten as:

$$\frac{dI}{dt} = \frac{1}{L_{load}} [(V_{source} - R_{load}I) - V_{arc}] \quad (4)$$

When arc fault occurs,  $dI/dt$  is negative, and then the current starts to decrease. When the gap length reaches the final value, a stable arcing is formed where  $V_{source} - R_{load}I = V_{arc}$  and  $dI/dt = 0$  as shown in Fig. 3 [8]. The stable operating point is point A instead of point B. For example, consider the case when the current experiences a small disturbance at point A, which causes a decrease. Because  $dI/dt > 0$  and  $V_{source} - R_{load}I > V_{arc}$ , the input power is greater than the power dissipated by arc. Therefore, the arc tends to burn more steadily, and the loop current increases back to point A. Similarly, when there is a small disturbance causing an increase in the current at point A,  $dI/dt < 0$  and  $V_{source} - R_{load}I < V_{arc}$ , and the input power is

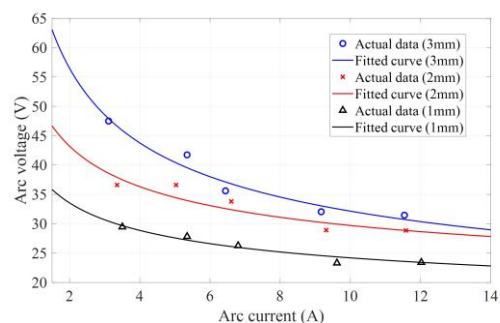


Figure 2: V-I characteristic under different gap lengths

less than the power dissipated by arc. Then the arc tends to extinguish, and the loop current decreases back to point A. Therefore, point A would be the stable operating point. Similarly, point B can be proved as the unstable operating point.

### Load Current and Source Voltage Effect

Because arc is a very complex physical phenomenon, it is difficult to analyze its behavior point by point because it cannot be exactly treated as a constant resistor. Therefore, the average arc resistance is calculated by averaging the arc resistance of each sampled data point in the first 2 seconds duration after the moving electrode has reached the predefined distance point. In Fig. 4(a), the average arc resistance and the amount of change in average resistance decrease as the load current level increases when the source voltage is fixed. On the other hand, it is fair to say that the DC voltage level has fewer impacts on the arc resistance compared to the load current level as shown in Fig. 4(b). The average arc resistance decreases slightly with increasing source voltage level as expected. Note that this condition is only satisfied when generating sustainable arcing. Also, arc resistance increases with increasing gap width, which agrees with Eq. (2).

## HF VARIATIONS IN DC ARC CURRENT

### Wavelet Packet Entropy

Wavelet packet decomposition (WPD) is a multi-resolution analysis that can divide a signal into different frequency bands. Entropy can be used to measure the degree of disorder. Wavelet packet entropy is achieved by combining WPD and entropy theory together. Specifically, after WPD analysis, the set of wavelet coefficients at  $j^{\text{th}}$  level and  $m^{\text{th}}$  frequency band,  $W_m^j$ , with values of  $\{w_{m1}^j, w_{m2}^j, \dots, w_{mn}^j, \dots, w_{mN}^j\}$  can be obtained, where  $m = 1, 2, \dots, 2^{j-1} - 1$  and  $N$  denotes the number of coefficients. Then, the entropy  $H_m^j$  can be calculated as follows:

$$H_m^j = - \sum_{n=1}^N p(w_{mn}^j) \log p(w_{mn}^j) \quad (5)$$

$$p(w_{mn}^j) = \frac{|w_{mn}^j|^2}{\sum_{n=1}^N |w_{mn}^j|^2} \quad (6)$$

where  $p(w_{mn}^j)$  is the probability of  $w_{mn}^j$ , and  $\sum_{n=1}^N p(w_{mn}^j) = 1$ . In this paper, the sampling frequency is 200 kHz, the WPD level is 3, and the analyzed window length is  $T = 40$  ms. Accordingly, there are 8 sub-bands with  $N=1000$  wavelet coefficients for each band. Daubechies 9 (db9) is used as mother wavelet because of its excellent performance in arc fault signal analysis [3].

### Characteristics of High Frequency Variations

Based on experimental observations, after initiation of arc

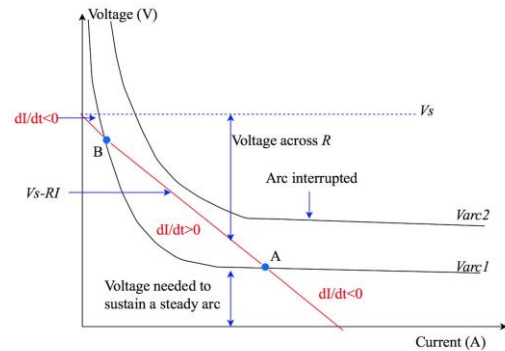


Figure 3: The conditions for a stable arcing point

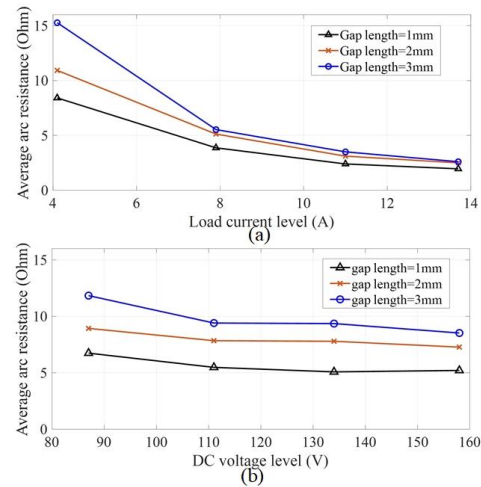


Figure 4: Average resistance under (a) fix current; (b) fixed voltage

fault, the arc behavior can be characterized in three phases as shown in Fig. 5:

- **Phase 1:** arc roots jump randomly and the shape of the arc column changes randomly. they cause dramatic variation in the current signal.
- **Phase 2:** arc roots jump randomly (but less frequently than that of phase 1). They show less variation than phase 1 with lots of spikes in the current signal.
- **Phase 3:** arc root tends to be stable at the edge of the electrode with less jumping and the arc column has a shape of bow. There are less variations and spikes in the current signal.

The frequency spectrum is shown in Fig. 6. The arc noise intensity in the current spectrum increases significantly after its occurrence. Furthermore, the spectrum level decreases when the phase shifts with time.

The wavelet packet entropy calculation is shown in Fig. 7. Right after the instant of arc initiation, the entropy for each band decreases significantly towards zero. This is mainly caused by the large spike introduced in arc current because of the arc ignition. After the initiation, the entropy of bands 2-4 and 6-8 shows some increase with little fluctuations, while that of band 1 and band 5 remains approximately the same but with larger fluctuations. Unlike the frequency spectrum, which changes significantly with different arc phases, the entropy of bands 2-4 and 6-8 remains

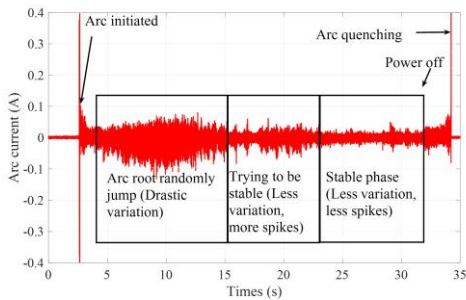


Figure 5: HF variation of DC series arcing at 11A/200V

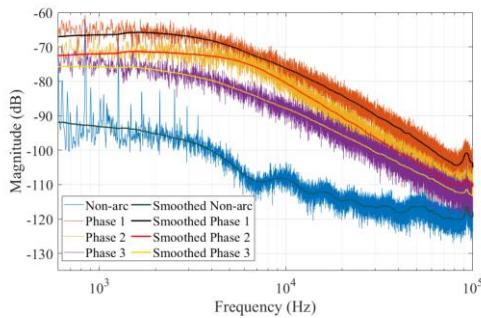


Figure 6: Average frequency spectrum of different phases

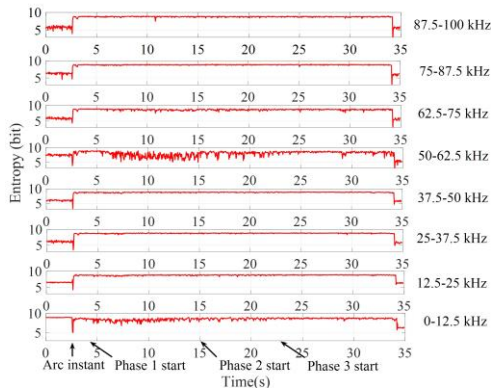


Figure 7: Wavelet-packet entropy (11A/200V, 1mm)

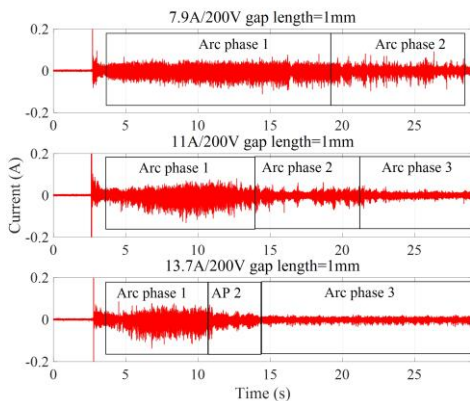


Figure 8: DC current dependency for different phases approximately unchanged. From the experiment, one can see that the higher the current, the faster the temperature rise in the arc column, and then the sooner arc phase 3 is reached as shown in Fig. 8. It also reveals the temperature dependency and preference. At higher temperature, the degree of thermal

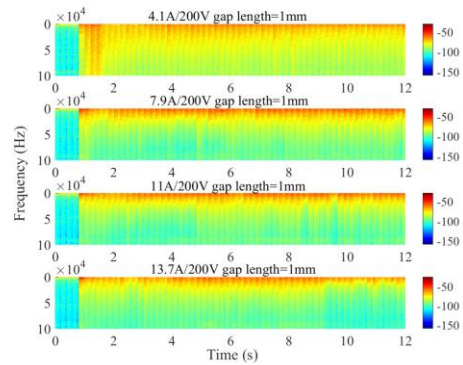


Figure 9: Current dependent arc spectrogram (fixed V)

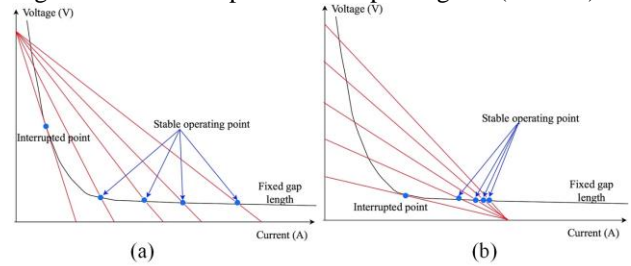


Figure 10: V-I curve for (a) fixed V; (b) fixed I

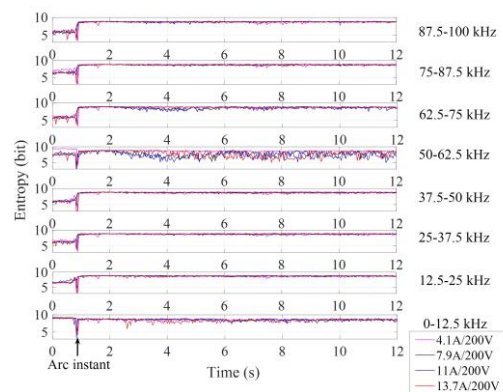


Figure 11: Wavelet-packet entropy under fixed V ionization of the metal vapor and mixed gases is higher.

**Current, Voltage, and Gap Length Effect**

As shown in Fig. 9, there are less high frequency variations at higher load current level under fixed voltage and fixed gap length. Additionally, when the load current level is higher, the stable operating point is much far from the interrupted point for the same V-I characteristic curve in Fig. 10 (a). It gives the stable operating point more margins, which accordingly increase the stability of the arc and thus introduce less variation in the arc current signal. The wavelet packet entropy calculation for different load current under fixed source voltage is shown in Fig. 11. The results are similar as discussed in the previous section. More importantly, the entropy of arc-state of bands 2-4 and 6-8 remains approximately unchanged when the load current changes. Similarly, there are less high frequency variations at higher source voltage level under fixed load current and gap length as shown in Fig. 10 (b) and Fig. 12. The higher

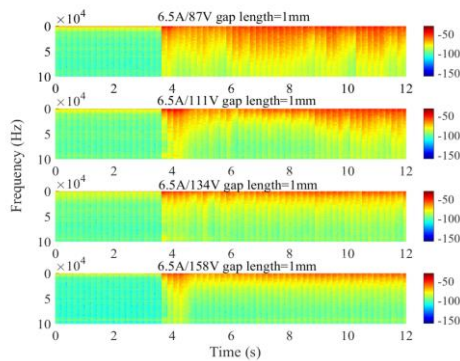


Figure 12: Voltage dependent arc spectrogram (fixed I)

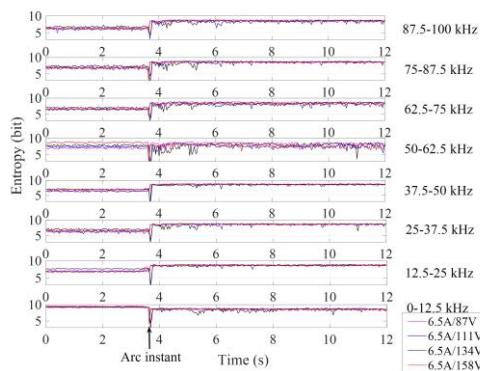


Figure 13: Wavelet-packet entropy under fixed I

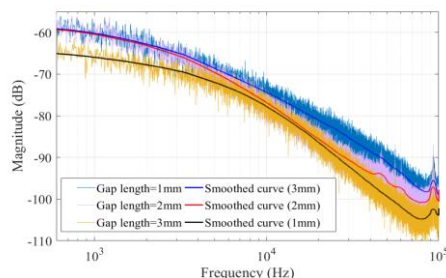


Figure 14: Average frequency spectrum at different gap lengths

source voltage gives arcing more margins to the interrupted point. Therefore, the arc is more stable and generates fewer variations at higher source voltage level. On the other hand, as shown in Fig. 13, the entropy of arc-state of band 2-4 and band 6-8 remains approximately same with the changing DC source voltage. In addition, In Fig. 3, with gap length increasing, the V-I characteristic changes and finally two curves intercept at the interrupted point. When the gap length exceeds the critical gap length, the arc will be extinguished. Therefore, it is expected that the high-frequency variation will be more significant at longer gap length as the stable operating point is closer to the interrupted point. As shown in Fig. 14, the gap length dependency has been revealed and the results are the same as expected.

## CONCLUSION

Based on experimental results, the following conclusions can be drawn:

1. The arc current and its spectrum show dependency on the source voltage, load current, and gap length. The arc fault tends to produce less arcing noise when the stable operating point is further away from the interrupted point. Therefore, when testing the effectiveness of arc fault detectors, the arc fault should be generated at high voltage and current level at a small gap distance to get the lowest arcing noise level to obtain the worst-case scenario.
2. Arc process can be generalized in different phases and the degree of variation in high-frequency components of the current is different under different experimental conditions. The higher the load current, the faster the arc reaches the final phase. The initial arc phase has the highest degree of variation.
3. Wavelet packet entropy can be used for fault detection purpose as it can extract a consistent pattern of arcing fault under arcing different conditions. There are clear changes of entropy before and after arc fault occurrence, and such entropy features of arc fault current could also be adopted for its more effective detection. Based on the experimental results, the frequency band of 12.5-50 kHz is recommended for fault detection purpose.

## REFERENCES

- [1] X. Yao, L. Herrera, S. Ji, J. Wang, "Characteristic Study and Time-Domain Discrete-Wavelet-Transform Based Hybrid Detection of Series DC Arc Faults," IEEE Trans. Power Electro., vol. 29, no. 6, June 2014.
- [2] "UL 1699B – Outline of Investigation for Photovoltaic (PV) DC Arc-Fault Circuit Protection," ed: Underwriters Laboratories, 2011.
- [3] S. Lu, B. T. Phung, and D. Zhang, "A Comprehensive Review on DC Arc Faults and Their Diagnosis Methods in Photovoltaic Systems," Renew. Sust. Energ. Rev., vol. 89, pp. 88-98, June 2018.
- [4] B. Novak, "Implementing Arc Detection in Solar Applications: Achieving Compliance with the new UL 1699B Standard," Texas Instruments, Dallas, USA, 2012.
- [5] G. Seo, J. Ha, B. Cho, and K. Lee, "Series Arc Fault Detection Method Based on Statistical Analysis for DC Microgrid," in Proc. IEEE Applied Power Electronics Conference and Exposition (APEC), Long Beach, CA, USA, Mar. 2016, pp. 487-492.
- [6] M. Zhen, W. Li, S. Qiangang, "The Characteristics of DC arc Faults Current," in Proc. European Conf. Power Electro. & App., Lille, France, Sep. 2013, pp.1-9.
- [7] S. Lu, B. T. Phung, and D. Zhang, "Study on DC Series Arc Fault in Photovoltaic Systems for Condition Monitoring Purpose," 2017 in Proc. Australasian Universities Power Engineering Conference, Melbourne, VIC, Australia, Nov. 2017, pp. 1-6.
- [8] P. G. Slade, Electrical Contact: Principles and Applications, Second edition, Boca Raton, Florida, USA: CRC Press, pp. 597-607.